nature portfolio

https://doi.org/10.1038/s41559-021-01487-z

Supplementary information

A 51,000-year-old engraved bone reveals Neanderthals' capacity for symbolic behaviour

In the format provided by the authors and unedited

A 51,000 year old engraved bone reveals Neanderthals' capacity for symbolic behaviour

Supplementary Information content

Supplementary information RESULTS
Supplementary information METHODS
Supplementary Figures 1 to 18
Supplementary Tables 1 to 9
Supplementary References

Supplementary information RESULTS

Site information

Einhornhöhle is a well-known Quaternary fossil site that has been frequented by treasure hunters since the Middle-Ages aiming to extract what they believed to be unicorn fossils. During the 18th century, geologists, palaeontologists, and later archaeologist became increasingly interested in Einhornhöhle due to abundant fossil finds. In 1925 a previously unknown cave part was discovered by the archaeologist Karl Hermann Jacob-Friesen who aimed to discover traces of Neanderthal occupations [49]. A large tunnel, measuring 35x 1x 1.5 m, was dug through *in-situ* sediments inside that gallery, but neither Neanderthal fossils, nor artefacts were discovered. However, when the first Middle Palaeolithic artefacts from Einhornhöhle were found in 1985 inside the Jacob-Friesen Gallery, it became apparent that the previous excavation had affected the two uppermost Middle Palaeolithic layers (D and E) over a distance of some 10 m in areas 1 and 2 (Supplementary Figure 1). Three excavation campaigns between 1986 and 1988 followed the new discovery whereby almost 200 lithic artefacts were retrieved [49-51] (Supplementary Figure 2). They are made of locally available raw materials such as siliceous slate, hornfels, greywacke, and quartzite, whereas flint was imported from >30 km away. In contrast, faunal material was abundant and was identified mostly from cave bear and various micro-fauna.

Since 2014, the authors have been conducting excavations inside the Jacob-Friesen Gallery that yielded six Middle Palaeolithic layers (D-I) beneath three archaeologically sterile ones (A-C). Previous observations in regards to lithic and faunal materials could be confirmed, while the lithic component is now more clearly attributed to Levallois flake production and

possibly to Quina flake production [46], which are typical flaking methods of the European Middle Palaeolithic.

Also excavations at a former cave entrance have been renewed in 2014, after a first test trench was dug in 1988 [49-51]. The major finds layers at this former cave entrance, layers 6 and 4.5, delivered cut-marked bones, a single bladelet fragment and the incised giant deer phalanx, the two latter coming from layer 4.5. Archaeological materials were thus first discovered through the renewed excavations.

Layer 4.5 likely correlates with layer B inside the cave (see sediment analyses in Supplement). However, layer B was deposited only 30-60 cm below the cave ceiling in areas farther inside the gallery (Areas 1, 2 and 5) (Supplementary Figure 1) and it lacks any archaeological finds. It would thus appear that Neanderthals only occupied the cave entrance area when the incised bone was deposited, possibly including the first few metres inside the cave (Area 3). Contrastingly, most of the cave's interior was hardly accessible. In any instance, the currently excavated volume at the cave entrance (Areas 3-4) is too small to permit an interpretation of the human occupation mode, settlement structure, or human activities. Only the faunal materials with apparent butchering marks and the incised giant deer phalanx shed some light on the human activities performed at this former cave entrance.

Stratigraphy and sediment analyses

Stratigraphy

The stratigraphy of the cave entrance can be summarised as follows (Supplementary Figures 3-5):

Layer 0 – Black/ dark-brown humus zone, ca. 0.3 m thick; sterile.

Cave entrance roof and walls consisting of dolomite

Layer 1 – Light-beige clayey silt containing 10-60 cm thick blocks, roots abundant, but decrease downwards, 0.5-1 m thick; sterile

Layer 2 – Beige to light-brown, partially laminated silt, some rootlets, 0.2-0.5 m thick; a single non-diagnostic flake at the boundary with layer 3, no bones preserved

Layer 3 – Brown to reddish-brown clayey silt containing lenses of rounded dolomite pebbles (1-2 cm diameter), some rootlets, 0.1-0.5 m thick; few bones

Layer 4 – Beige clayey silt containing abundant rocks (10-30 cm diameter), some rootlets, 0.5-0.8 m thick; some bones, no artefact

Layer 4.1 – grey-brown clayey silt containing small rocks (up to 20 cm diameter), few rootlets, 1m thick but only 20 cm wide showing clear signs of sloping; few bones

Layer 4.5 – Brown to grey-brown clayey silt containing lenses with rounded dolomite pebbles (1-2 cm diameter) and small rocks (up to 10 cm diameter), some rootlets, 0.1-0.5 m thick;

bones are abundant, some with cut-marks, single bladelet fragment, single engraved bone (find no. 423)

Layer 5 – Reddish light-beige clayey silt containing some rocks (10-20 cm diameter), no rootlets, 1.5 m thick; some bones, few with cut-marks

Layer 6 – red clayey silt containing some rocks (10-20 cm diameter), no rootlets, 0.5 m thick; bones are abundant, some with cut-marks.

Layer 7 – Beige clayey silt containing abundant rocks (10-30 cm diameter), >0.5 m thick; present c. 3 m east of the west section, base not reached; few bones; single bladelet with two ridges.

Sediment analyses

The median grain size (P=50) for all sediment samples are within the silt fraction (25.9 to 8.8 µm) and characterized as clayey silt with low fine-sand contents between 17.7 % and 4.4 % (Supplementary Figure 5). Layer 4.5 where the engraved bone was found shows a multi-modal grain-size distribution with peaks at 15 µm, 25 µm, and a minor peak around 125 µm (samples 928 and 929). The latter minor peak around 100 – 130 µm is present in all samples and may point to a minor portion of aeolian sand import into the initial material when it was exposed to the former land surface. However, this needs to be confirmed by investigation of the particle's surfaces. This was not performed yet.

Within all samples dolomite is the dominant mineral and quartz the second-most mineral. Calcite is present in varying amounts in all samples except for samples #927 and #926 which are calcite-free. Highest portions of calcite are found in samples #928 and #929 from layer 4.5 where the engraved bone was found. In layer 6 – represented by samples #926 and #925 – also bones were found but only the lower sample #925 near the bone finds contained calcite. This may show that the higher calcite contents could be responsible for good bone preservation. A detailed clay mineral identification was not performed, but chlorite and muscovite/illite were identified with highest abundances in samples #928 and #929 (layer 4.5) which points to the relative high Weathering Index after [68] with values around 88. In accordance with a high weathering intensity in layer 4.5 the siliceous-rich and aluminium-rich minerals (orthoclase, anorthite, and quartz) are enriched.

The TOC content is generally low (<1 %) as a result of intense weathering and degradation of organic matter (Supplementary Figure 5). The phosphate contents show relatively low values (< 2 mg/g) and roughly parallel the TOC values. The TIC ranges between 6.9 to 10.9 % due to the high dolomite and calcite contents.

The Weathering Index is consistently high with values between 82 and 91, peaks in samples #925 and #926 (layer 6), and the lowest value in samples #922 (layer 5). From the top of the

profile (pH 8.2) to the base (pH 7.5) the pH shows weakly alkaline conditions, which is due to the high buffer capacity of the dolomitic and calcitic layers.

Layer 4.5 probably correlates with layer B inside the Jacob-Friesen Gallery where this layer shows a pH of 7.4 (weakly alkaline conditions) and also represents clayey silt with a medium grain size (P=50) between 17.9 to 23.4 µm. The mineral content also exhibits high calcite contents and enrichment of orthoclase, anorthite, and quartz.

Fauna and taphonomy

The giant deer is the third most represented taxa (NISP = 12; MNI = 1). All specimens are teeth – 1 incisor, 3 premolar, and 6 molars – except for the engraved second phalanx (inv.-no. 46999448-423; Figure 1) and an unmodified second phalanx (Supplementary Figure 6). The unmodified bone was found in the same stony sediment pocket of layer 4.5 just 30 cm SSW of the modified item and does not bear any cut-marks or incisions. Both phalanges might come from the same individual and possibly even from the same limb.

While many of the observed bone surface modifications (BSMs) on layer 4.5 materials associable to human agency are typical (AM in Supplementary Table 1; are Supplementary Figure 7), some were considered atypical in terms of low occurrence per bone, anatomical position on the element, shape, and/or width of the linear mark (pAM in Supplementary Table 1). A similar situation was recorded for carnivore damage (pCM in Supplementary Table 1). For these reasons, the modifications were sorted into four groups. Anthropogenic linear marks are reported as AM (anthropogenic modification) when certain, or as pAM (potentially anthropogenic modification) when likely. Accordingly, taphonomic signatures of carnivores are referred to as CM (carnivore modification) when certain, or as pCM (potentially carnivore surface modification) when likely.

The state of preservation of cortical bone surfaces is generally good, showing a low rate of advanced weathering (%NISP = 6.5) (Supplementary Table 2). Most fossils only display linear cracking, and surface modifications are well visible. This is also true for the engraved giant deer second phalanx that additionally displays localised edge chipping. By contrast, in some specimens, notably those found near the wall face, a significant part of the surface is damaged by root etching and, therefore, possible modifications are no longer visible. Many of the bones are complete or near-complete suggesting low in-situ attrition, and the few fragmented specimens appear to be the consequence of root etching and/or sediment pressure. No evidence of heat exposure was observed.

Inclination and orientation

The orientation data shows tendencies towards northern and eastern directions in the northern part of the excavation, mostly for bones in layer. 4.5 (Supplementary Figure 8). Also southerly directions are well represented here interrupting zonal patterning. An equally heterogeneous picture results from finds in layer 6. The incised bone is oriented in an NNW-SSE direction.

The pattern obtained from the former cave entrance of Einhornhöhle reflects multi-orientation. Mono-orientation on the other hand can result from sediment movement, e.g. along slopes and through cavities, or from water streams, whereas multiple directions can be the result of various agents including humans and animals [52].

The inclination data of layer 4.5 shows low values (< 25°) for its upper and northern parts, whereas lower portions show higher values (> 25°). High inclination values (> 45°) represent layer 6 finds, especially in its southern and central parts, whereas the northern fringe shows low values (< 25°). Similar to data of its immediate surrounding, the humanly modified bone shows a low inclination value of 11.6°.

Inclination and orientation data show that the surroundings of the engraved bone seem relatively *in-situ*, whereas other parts of layer 4.5 and layer 6 in particular, show clearer signs of sloping.

The incised giant deer second phalanx (inv. no. 46999448-423)

Châine opératoire

The following *châine opératoire* is suggested for the modified giant deer phalanx: Neanderthals carefully disarticulated the phalanx, probably from a hunted giant deer. In the next step, the phalanx was cleaned from tissue and probably boiled for some time, which required the use of fire for boiling. After drying, the bone was carved, probably in a continuous process within c. 90 mins, although a longer time span, e.g. over several days cannot be ruled out.

The giant deer second phalanx might have been collected, rather than obtained from a freshly hunted animal, and processed after some time of decay. As recent studies have shown however, putrefying liquids of decaying bones limit the efficacy of cutting [60] making the usage of a withered bone less likely. Also, the presence of a further giant deer phalanx bone, as well as, giant deer teeth at the site, make active hunting seem a more likely scenario. Both actions, collecting raw material and hunting, involve behavioural premeditation.

Post-depositional alterations

The engraved giant deer second phalanx displays different localised post-depositional alterations (Figures 3-4, Supplementary Figure 10) that primarily affected the left side of the engravings (lines 1-3). An ancient surface abrasion of unknown origin covers parts of the surface adjacent to line 1 and extends onto line 2. It altered the incisions' vertical surfaces and profiles that probably were deeper before. Two elongated depressions that compacted the left area of line 2 might represent bite marks caused by a small carnivore (Supplementary Figure 10). Exposed cancellous bone is visible on lines 3 and 6. Their colouring and slight rounding support a classification as 'ancient' and might be caused by trampling, sediment pressure and/or weathering. The horizontal surface of line 3 shows ripples and micro chipping which may have been caused by repeated scraping motions with varied force, or by post-depositional pressure. The vertical surface remained intact. Half of line 6's original horizontal surface is preserved while the remainder shows exposed cancellous bone. Thus, inferences on the line's minimal depth and horizontal extension can still be made (Figures 3 and 4). Small pits observed on both epiphyses are related to carnivore attrition. Finally, edges and surfaces appear locally rounded and micro chipping is visible in some places. The only distinctively modern damage on the modified bone is a linear scratch at line 3 that was likely caused by an excavation tool.

While post-depositional alterations thus left different localised traces on that item, the overall patterning of the incisions remains clear and the corpus of surfaces, profiles, and work traces forming these lines, particularly those of lines 1-2 and 4-5, respectively, are well visible. The bone’s state of preservation is comparable to other bones from the same layer (Supplementary Table 2). Human agency may account for some of the observed surface rounding and micro chipping in the case the item had been worn or carried for an extensive time before it was deposited at Einhornhöhle's cave entrance. Alternatively, the same traces might have been caused by engraving, weathering, sediment pressure and/or trampling. Therefore, the causative agent remains elusive.

Experiment

The five different bone pre-treatment approaches considerably modified their workability.

Cleaning: Fresh bone proved difficult to remove soft tissue from, as the slippery, greasy surfaces made controlled tool use almost impossible. Cutting/scraping (c. 20 mins) to expose most of the bone led to various unintentional cut marks. Dried bone proved slightly easier to clean (c. 1-2 mins to remove most tissue), with small amounts of soft tissue remaining. Cooked bone had most soft tissue removed as a result of the cooking procedure, any remaining amounts could easily be removed.

Cutting and scraping: Fresh bone proved extremely difficult to cut and scrape due to the greasy, slippery surface and the extremely hard bone tissue. On dried bone, vertical cuts were easy at first, but increasingly more difficult with greater depth due to the hard bone tissue. Horizontal scrapes were almost impossible to achieve on both dried bones while sticky, tattered, hardened soft tissue remains resulted in an immense absorption of cutting force and a loss of blade control. Only scraping was used on Bone 4 (1 x cooked), which proved easy but did not create the very sharply defined grooves. Bone 5 (2 x cooked) was carved with a combination of alternating vertical cuts and horizontal scrapes and resulted in well-defined, progressively deeper grooves. The cooking process resulted in an almost mellow surface allowing easy and precise carving. The alternation stopped the blade at the bottom of the groove and prevented overshooting, but also caused break-outs and/or a rounded upper edge of the cut.

Blades: On fresh bone, blade control was extremely poor due to the slippery tissue and surface. Little macroscopic wear could be found on this blade. On dried bones, well-developed wear and some edge splintering formed on the blades. The cooked bones resulted in heavily worn and partially dull blade edges after c. 10 mins of use. Worn, serrated edges in some cases caused an uneven surface on the bone which had to be smoothed with a fresh blade.

Results: Fresh bone proved completely unsuitable and the attempt was declared unsuccessful after 25 minutes. The dried bones were partially successful with two 1 mm deep grooves (Bone 2, c. 13 mins and c. 7 mins processing time), one irregular, shallow groove (Bone 3, <0.5 mm, c. 15 mins) and one 1.5 mm deep groove (Bone 3, c. 8 mins). Boiled bone proved extremely suitable for groove carving, as the clean, mellow surface allowed easy cutting and scraping as well as excellent blade control and a firm grip. Four 2 mm deep grooves could be carved with processing times of 10 mins and 6 mins (Bone 4) and 11 mins and 10 mins (Bone 5) respectively.

Conclusion: Twice boiled, thoroughly cleaned bones proved to be the most suitable material for carving grooves with a depth of 2 mm. The mellow surface and lack of slick/greasy tissue allows for easy cutting and a firm grip. A combination of cutting and scraping motions has proven most successful. Dried bones with soft tissue remains proved significantly less suitable as blade control is lost and the bone tissue remains significantly harder, leading to an increased expenditure of time and shallower grooves (around 1 mm depth). Fresh bone appears to be completely unsuitable as the greasy, slippery surface leads to a total loss of blade control. Whilst the surface, once reached, can be cut relatively easily, the hardness of the bone tissue makes scraping almost impossible.

The results are consistent with previous experiments on cutting decaying bone [60], whereby meat remains and putrefying liquids had a negative impact on bone handling properties causing tools to slip. In contrast, whenever less organic tissue was attached to the bone,

wider and deeper incisions had been observed. Both observations compare well to our experimental results.

Regional context

The engraved bone item from Einhornhöhle was found in context with cut-marked faunal remains at a former prehistoric cave entrance that later eroded and was filled in with sediments. In the absence of diagnostic lithic finds, the engraved bone is attributed to Neanderthals through absolute dating. Additionally, six superimposed Middle Palaeolithic layers with stone artefacts found some metres inside the cave confirm the repeated presence of Neanderthals during the Weichselian (Supplementary Figures 1-2). The surprisingly early date (>55–47.5 ka calBP, 2-sigma) of the engraved phalanx is in good agreement with further radiocarbon dates from the same and the underlying layer (Supplementary Table 8; Supplementary Figure 14).

The find from Einhornhöhle is not the only object demonstrating advanced technology and advanced behaviour among Neanderthals in northern Central Europe (Supplementary Figure 16). A number of late Lower Palaeolithic and Middle Palaeolithic sites located at the northern periphery of the world inhabited by early humans produced evidence for advanced technology (wooden weapons, bone tools and adhesives) [17-23, 26-27] and now a giant deer phalanx engraved with a complex line pattern. Whether this is solely related to outstanding preservation conditions at some of these sites is questionable as palaeo-lakes (Schöningen, Neumark-Nord), cave sites (e.g. Einhornhöhle, Feldhofer Grotte, Balve Cave) or open-air sites with good faunal preservation (Salzgitter-Lebenstedt) are presumably found in a number of localities across Eurasia. Despite its peripheral location, the region seems to have presented fruitful grounds for novel technologies and innovative thinking in *pre-Homo sapiens* hominins.

Supplementary information METHODS

3D digital microscopy

The 3D reflected light microscope Keyence VHX-5000 (Keyence, Neu-Isenburg, Germany) was used for non-destructive, high depth-of-field, and 3D images at different magnifications. The microscope is equipped with a VHX-ZST dual objective zoom lens. In this study, the zoom lens VHX-ZS20 was used enabling magnifications from 20× to 200×.

To examine the engravings of the bone (inv. no. 46999448-423), images of the observation fields were captured at magnifications of 20×, 50×, and 100×. At these magnifications, images in 2D and 3D were taken by means of single image capture and image stitching. Up

to 36 individual images were combined to create a stitched image. Single images of the observation fields were taken at the centre of the engravings whereas the stitching procedures enabled the observation of the entire engravings. For 3D images, the lowest focus plane of the observation fields was manually determined. Then, using automatically acquired images in focus at different planes in Z-direction (i.e., height), the microscope produces a 3D reconstruction of the observation field. Through this method, topographic profiles of the 3D representation of the engravings were obtained. The colour mapping codes the 3D image according to its height within the 3D representation. Blue designates the lowest focus point, whereas red codes the highest focus point. With the use of such 3D images, topographic profiles of the 6 engravings were produced. The cross-sectional profile-line measurements were conducted by a straight line intersecting the engravings perpendicularly. The measurement position was displayed by a profile graph in the respective images.

Fauna and Taphonomy

The identification of the faunal remains was carried out using the skeletal reference collection at the Institut für Naturwissenschaftliche Archäologie Tübingen following standard protocols for the identification of large ungulates [69-70] and for the identification of bears [71]. To avoid the problem of data aggregation and given the relatively low fragmentation rate, the NISP (number of identified specimen) was used to determine species abundance [72-74]. General animal categories have been identified [73] and adjusted to taxonomy and body mass of Pleistocene species from central Europe.

The characterisation of the bone surface modifications (BSM) was done in accordance with established protocols [75-76] while the characterisation of the carnivore damage was conducted following work published by Fernandez-Jalvo & Andrews [77]. Taphonomic observations of surface preservation and modification were categorised in compliance with standard literature [73-74, 77-78].

All bone surface alterations were identified at varying magnification levels using a magnifying glass (mobilux LED x10) and the ZEISS Stemi 305 Greenough stereo microscope with magnification range 0.8x - 4.0x.

Sediment analyses

Sediment samples were collected form the western main section during the excavation (Supplementary Figure 5). Sample size of the 10 samples was about 200 g each. Where possible, two samples per layer have been retrieved in order to assess within-layer variability. All samples have been 3D-recorded with total station (Leica TS06-ultra2).

Grain size analyses were performed for the fraction < 1 mm with a laser diffraction particle size analyzer (LS13320 PIDS Beckman-Coulter) after acid treatment (15 % HCl) to eliminate carbonates and $Na_4P_2O_7$ (sodium diphosphate) as anti-coagulation. From the prepared sample, two control samples were measured each with three independent runs. For the interpretation, the average of all six measurements per sample were calculated.

For the identification of the mineral composition x-ray powder diffraction was applied with a RIGAKU Miniflex600 at 24 mA/36 kV (Cu kα) from 2° to 80°(2θ) with a goniometer step width of 0.02°(2θ) and a step velocity of 0.5°/min. For the identification and semiquantitative mineral composition the software program X-Pert HighScore Version 1.0b by PHILIPS Analytical B.V. was used.

Total carbon (TC) was determined with an elementary analyzer (LECO TruSpec CHN Macro). For the determination of the TIC (total inorganic carbon) content CO_2 was evolved during hot (70°C) acid (H_3PO_4) treatment and quantified conductometrically. The TOC (total organic carbon) content was calculated by subtraction of TIC from TC.

Elements (Al, Ca, Fe, K, Na, Mg, Mn, P as PO_4) were measured by ICP-OES spectrometry (Perkin Elmer Optima 2100 DV) after aqua regia solution of c. 1 g of homogenized sediment of the < 2 mm fraction (DIN EN 13346) [79].

The weathering index (WI) was calculated according to Nesbitt and Young [68] who use the following formula: $Al_2O_3/(Al_2O_3+Na_2O+K_2O)*100$. Higher values reflect increasing weathering influence and enrichment of aluminum and quartz. The pH value was measured using the unprocessed air-dried <2mm samples and determined in aqua dest and 0.01 M CaCl2-solution according to DIN ISO 10390 [80].

Inclination and orientation

During the excavation, the incised bone was 3D recorded *in-situ* using an EDM total station (Leica TS06-ultra2). Two coordinate points were taken at the base of the incised bone recording the deposition level along its longest axis (X1: 5721298.853, Y1: 597097.077, Z1: 381.139; X2: 5721298.913, Y2: 597097.057, Z2: 381.151; WGS 84, UTM zone 32N). The same procedure was applied for all single finds. Bones > 3 cm, teeth and lithics > 2 cm were thus 3D-recorded with a total station taking two points at each item. Smaller objects were recorded with one point each. The purpose of the two-point levelling was to later use the data in a GIS to calculate inclination and orientation data for the whole assemblage.

The total station data was processed in QGIS 3.8.2. Individual 3D-cooordinates were allocated by specimen (e.g. three 3D-coordinate points can belong to one and the same bone). QGIS's angle measuring tool was used to calculate the angle between individual points in order to obtain orientation data that is then translated into cardinal points following

the northernmost point (e.g. a bone with an orientation of 45° has a NE-SW orientation translated into NE).

In order to assess the inclination of the finds, the csv.file was re-uploaded into GIS and the X-coordinate replaced by the Z-coordinate. This was done to illustrate altitude data on a plain surface. Thereafter, the same angle measuring tool was applied as for the orientation data. Both newly created information (orientation and inclination) were edited into the existing dataset for every find ID.

In order to obtain a density-distribution model, the centroid of multiple points representing a single find object was calculated. This centroid point still containing all previous information was then used to calculate the Inverted Distance Weighing (IDW) model. 'Power' was raised to 5 to smoothen data gaps. Low inclination values would speak for a relative *in-situ* location of finds, whereas high values make redepositing more likely.

Experiment

Topic: Flint blades were used to manually carve grooves into cattle bones, similar to the incisions on the giant deer phalanx (no. 46999448_423). These consist of distinctive evenly stepped, vertical planes combined with groove planes horizontal to the bone surface (Supplementary Figure 14).

Research question: 1. Which techniques were used to create the grooves? 2. What are the best conditions to easily (carving time, groove depth, success) carve the grooves?

Experimental setup: Five phalanges (phalanx media) of an 18-month-old Limousine cattle were obtained from a local slaughter house within two hours of slaughtering. At the slaughterhouse, the bones were kept at 2°C and further processing began within one hour of collection. The bones were treated in five different manners and stored for two days prior to the experiment:

Bone 1: as fresh – soft tissue mostly removed, in plastic bag in a fridge at 2°C

Bone 2: room dried – soft tissue mostly removed, c. 20°C in stable environmental conditions

Bone 3: open air dried – soft tissue mostly removed, varying temperatures c. 4°C-25°C

Bone 4: 1 x cooked – boiled in plain water for 1 h, most tissue removed after cooking, room dried

Bone 5) 2 x cooked – boiled in plain water for 1 h, most tissue removed after first boil, boiled again in plain water for 1 h, remaining tissue removed, air dried

Purpose-made flint blades were obtained, recorded (photographed, length, width, thickness and weight) and used to work the bones (Supplementary Figure 13 and Table 6). The blades are made of Baltic flint that is available some 30km north of Einhornhöhle while flint tools and chips have been reported from Middle Palaeolithic layers inside the cave [50-51]. The blades

used during the experiment are 5-8 cm long, 0.2-0.3 cm wide and weigh 6-8 g. Two different methods were used to create each groove:

A) Cutting – to create vertical planes

B) Scraping – to create planes horizontal to the bone surface

Each bone was allocated two individual blades, each blade was used with both techniques – cutting and scraping. At a later stage, this will allow us to match thus potentially created wear marks to the different conditions of bone preparation. The aim was to create grooves with a depth of 2 mm.

Recording: All bones and flint blades were photographed prior to the experiment. Working shots were taken during the carving process. The time it took to create each groove was noted; empirical observations were discussed and recorded.

Rational: Prior to the experiment, we ruled out chopping as a technique to create the incisions. Chopping as a high-energy-impact technique can be expected to cause compaction and crushing of bone tissue [57] that would have been visible at the base of the engravings on the giant deer phalanx. This was not the case, and was observed neither during stereo-microscopy, nor in µCT scans, nor during 3D digital microscopy, with the sole exception of line 3. The horizontal plane of line 3 shows a linear crack that is macroscopically visible. However, the crack is connected to modern excavation tool damage as it is accompanied by non-patinated white cancellous bone.

Given the size of the incisions (15-30 mm in length, 2-5 mm deep) a very small, but heavy tool would have to be used, likely causing uncontrolled cracking and splintering of bone surfaces and engravings while risking major loss of bone substance [81-82]. There are also anatomic limitations when hand-holding small objects (the carved bone is c. 6 cm long) while applying intense force, making controlled incisions nearly impossible. For all these reasons, we decided to turn towards more controlled engraving techniques and as the experiments shows, the chosen technique is highly replicative of the observed traces (Supplementary Figure 14).

To test whether soaking bone in water for a prolonged time would soften the surface layer thus enabling easier carving, a piece of twice cooked, fully defleshed cattle long bone was cut in two, and one half was submerged in water for six weeks. Afterwards, flint blades were used to make a series of test cuts in each piece to check whether the soaked bone would be easier to cut. After multiple cuts in each bone no difference in hardness could be detected. Other experiments have shown that water submersion works to soften thin or fragmented bone pieces, up to a maximum thickness of 2.5 mm (e.g. [83-84]), whereas the engraved item is up to 39.9 mm thick. Although carving properties could be expected to be similar to bone cooked twice, we only selected the phalanx bones during the experiment to allow for systematic comparison.

Radiocarbon samples (Pre-treatment and dating procedures)

All laboratories involved apply somewhat deviating pre-treatment and dating protocols. Available information is however iterated below.

Leibniz Labor Kiel

A general overview on pre-treatment and dating procedures can be found on their website: https://www.leibniz.uni-kiel.de/en/ams-14c-lab/reporting-of-results?set_language=en

Their procedure for the radiocarbon dating of the engraved phalanx (inv-no. 46999448-423) is described in the following. The phalanx was sampled on the opposite site of the carved surface using a Dremel corer device. Sampled material consists of powdered trabecular bone material from the inside (app. 500mg), which was first demineralised with HCl (c. 1%) and then treated with 1% NaOH (20° C, 1hr) to remove humic acids. A second hydrochloric acid extraction (1%, 20°C, 2h) was applied to eliminate atmospheric carbon dioxide which may have been introduced during the alkali step. The organic residue was gelatinized in demineralized water at 85°C and pH=3. Non-soluble organics were filtered through a 0.3µm quartz fibre filter and discarded, and the remaining gelatin (collagen) was lyophilised thereafter (modified Longin-method [85]). Collagen was burnt to CO^2 at 900°C together with CuO and Ag in an evacuated quartz ampoule. The resulting CO^2 was graphitized with H^2 and iron powder as a catalyser at 600°C. The iron-graphite-mixture was then pressed into an aluminium sample holder for the AMS measurement. The ^{14}C content was measured in a 3 MV HVEE Tandetron AMS-system. The isotope ratios $^{14}C/^{12}C$ and $^{13}C/^{12}C$ of the sample were measured simultaneously and compared to the CO^2-measurement standard (SRM 4990C, Oxalic acid-II). Effects resulting from recent radiocarbon contamination were corrected via double-blind-test.

The resulting ^{14}C ratio of the sample is then first corrected for isotope fractionation [86]. In a second step, measured sample radiocarbon concentrations are corrected for process blanks (i.e. background correction), resulting from the measurement of “infinitely” old samples such as geological bone sample material > 100 ka. The final sample ^{14}C concentration is related to the hypothetical atmospheric value in 1950 and denoted as pMC (percent Modern Carbon).

A conventional ^{14}C-age was calculated from this value according to [87]. The uncertainty of the ^{14}C-result respects uncertainties in $^{14}C/^{12}C$ ratios of the sample and measurement standards, the uncertainty of the corrected isotope fractionation and the uncertainty of the blind value.

On average, normal carbon-sized bone background samples give apparent ^{14}C concentrations around 0.2 ± 0.07 pMC (percent Modern Carbon), equivalent to 49,800 ^{14}C years BP. After blank correction, sample KIA55192 gave a radiocarbon concentration 0.26 ± 0.08 pMC, equivalent to a finite radiocarbon age of 47,800 +2,800/-2,100 BP. The resulting

^{14}C-age was calibrated with the OxCal 4.4.2 calibration software using the IntCal20 calibration curve [61-62].

While pre-treatment protocols and dating methods differ between radiocarbon laboratories, the Leibniz Labor Kiel has demonstrated to produce age estimates similar to other well-established laboratories, such as CIO (Groningen) and ORAU (Oxford) [88], which underscores the reliability of the finite age obtained from the incised bone.

CEZA Mannheim

The following is a summarised translation from their results report. Collagen was extracted via modified Longin-method [85], the fraction >30kD was then separated via ultrafiltration and lyophilised. After pre-treatment, the remaining sample was burnt to CO^2 in an elemental analyser and the CO^2 fraction catalytically reduced to graphite. The ^{14}C content was measured in an AMS-system type MICADAS. The isotope ratios $^{14}C/^{12}C$ and $^{13}C/^{12}C$ of samples, calibration standards (Oxalic acid-II), blanks and control standards were measured simultaneously in the AMS system. Resulting ^{14}C-ages are normalised at 13C=-25‰ [87] and calibrated with the OxCal 4.4 calibration software using the IntCal20 calibration curve [61-62].

CIO-Groningen

A general overview on pre-treatment and dating procedures can be found on their website (https://www.rug.nl/research/centre-for-isotope-research/research-and-projects/main-research/isotoop-datering/) while a detailed account of currently used equipment and applied procedures has been published recently [89].

Poznan AMS Laboratory

The full procedure description is available online: https://radiocarbon.pl/en/description-of-procedures/

Supplementary Figures

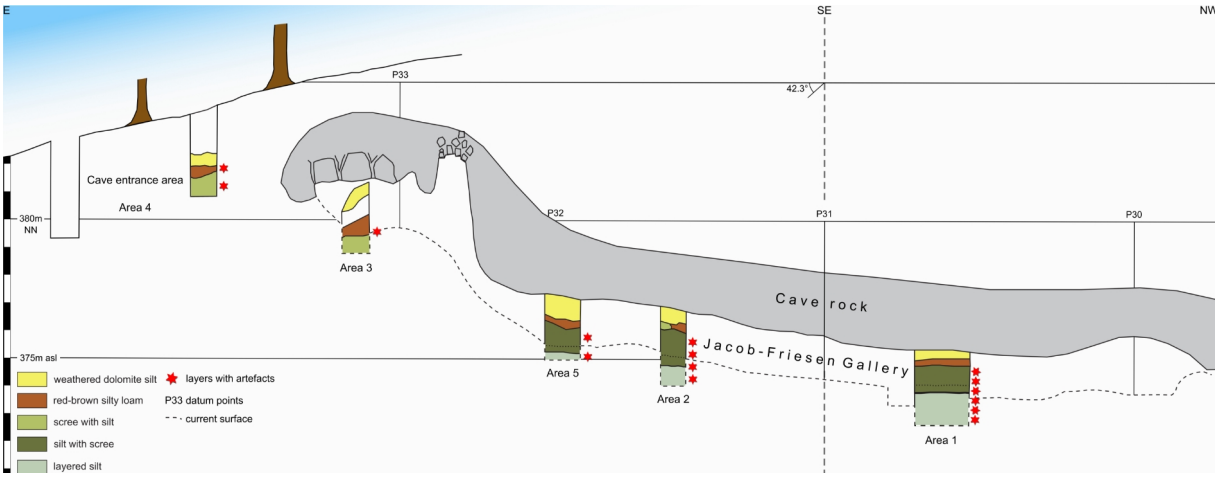

Supplementary Figure 1. Einhornhöhle. Section through the Jacob-Friesen Gallery with the cave entrance area (Area 4) to the east (left). See Supplementary Figures 3-4 and Figure 2 of the main text. Changed after [50].

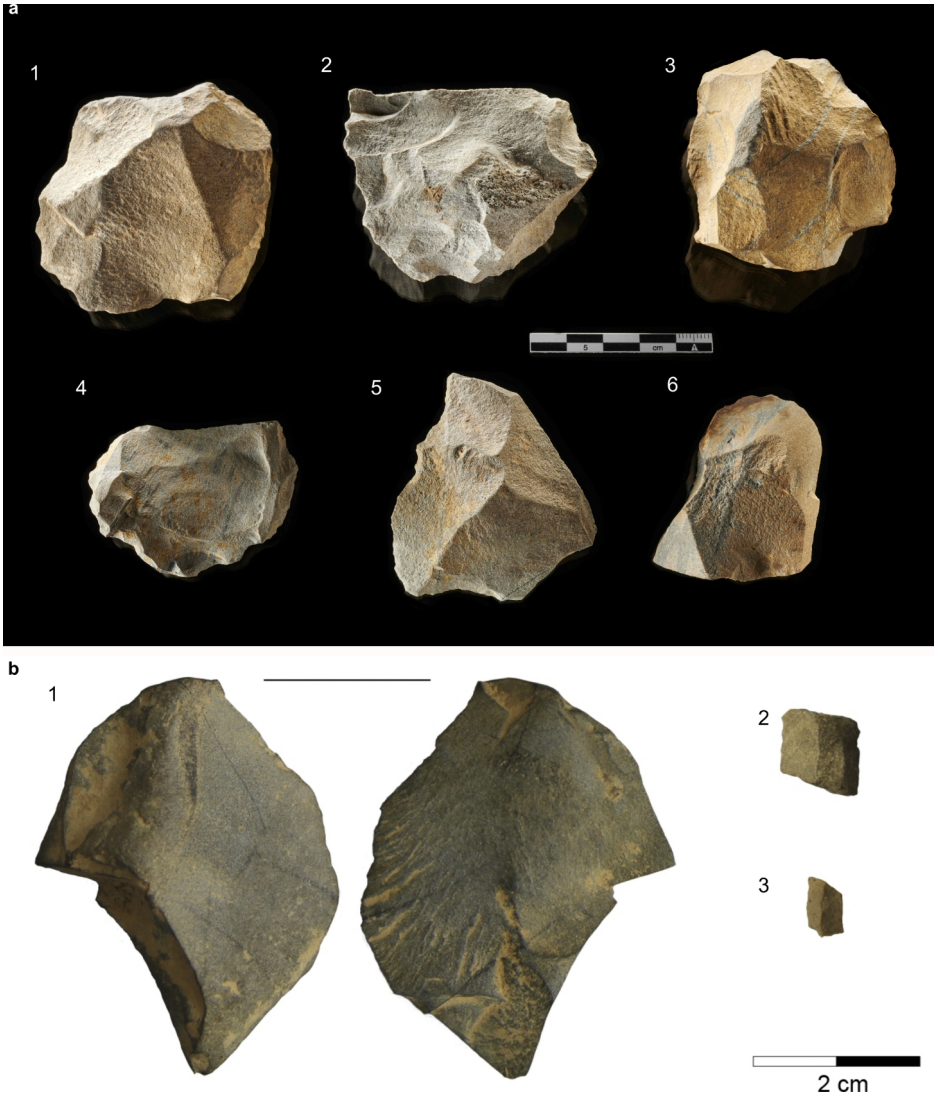

Supplementary Figure 2. Einhornhöhle. Lithic artefacts. **a** Lithics from the Jacob-Friesen Gallery. (1) Levallois preferential core. (2) Biface fragment. (3) Levallois centripetal core. (4-5) Levallois flakes with retouched edges. (6) Flake with distal wear. **b** Lithics from the former cave entrance. (1) Cortical flake form top of layer 3. (2) Bladelet fragment from layer 7. (3) Bladelet fragment from layer 4.5

Supplementary Figure 3. Einhornhöhle. Cave entrance area (Area 4). Snap shot taken towards the end of the excavation showing partially exposed main features.

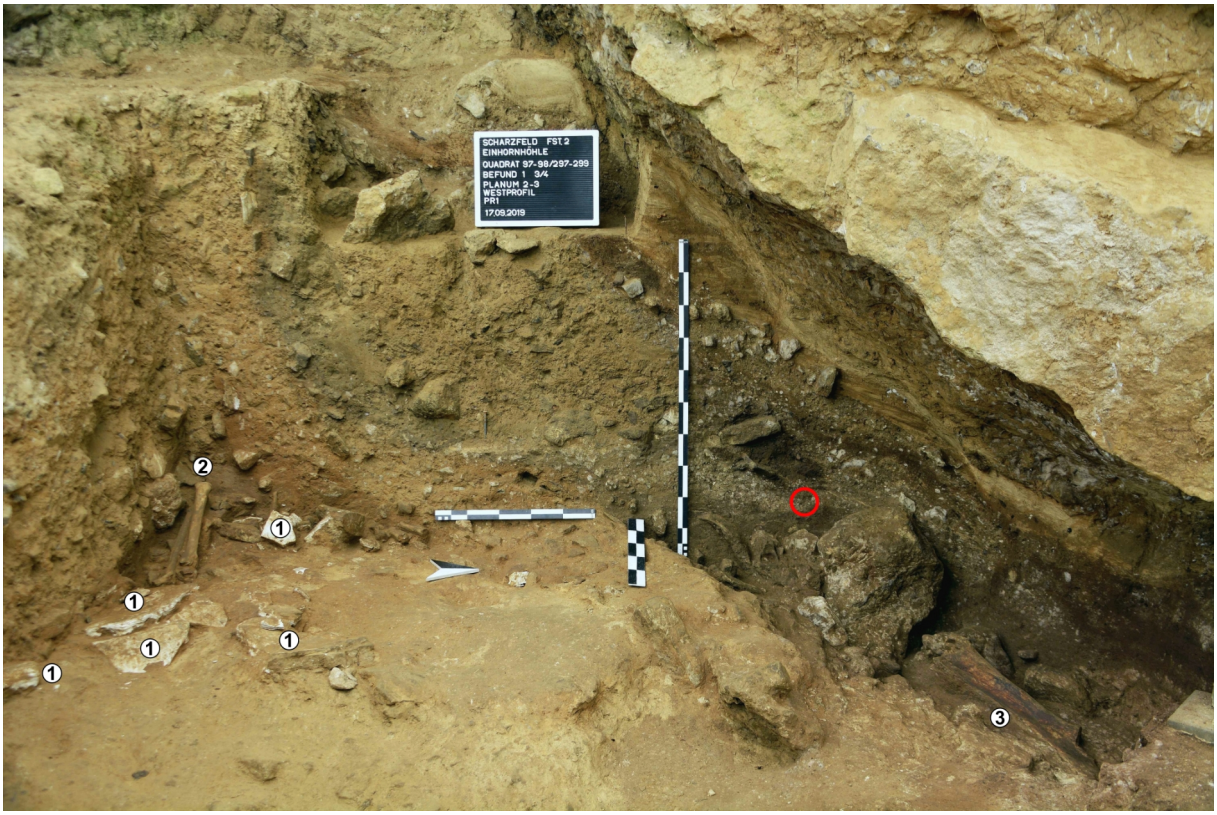

Supplementary Figure 4. Einhornhöhle. The main section (west section) at the cave entrance. The northern entrance wall is visible to the right, while the southern entrance wall would be about a metre to the left (Supplementary Figure 3). Red circle: Projected location of the engraved bone (inv. no. 46999448-423) in layer 4.5. (1) Horizontal calcrete slabs. (2) Partially articulated red deer bones in layer 6. (3) near-horizontal bovid bone in layer 4.5.

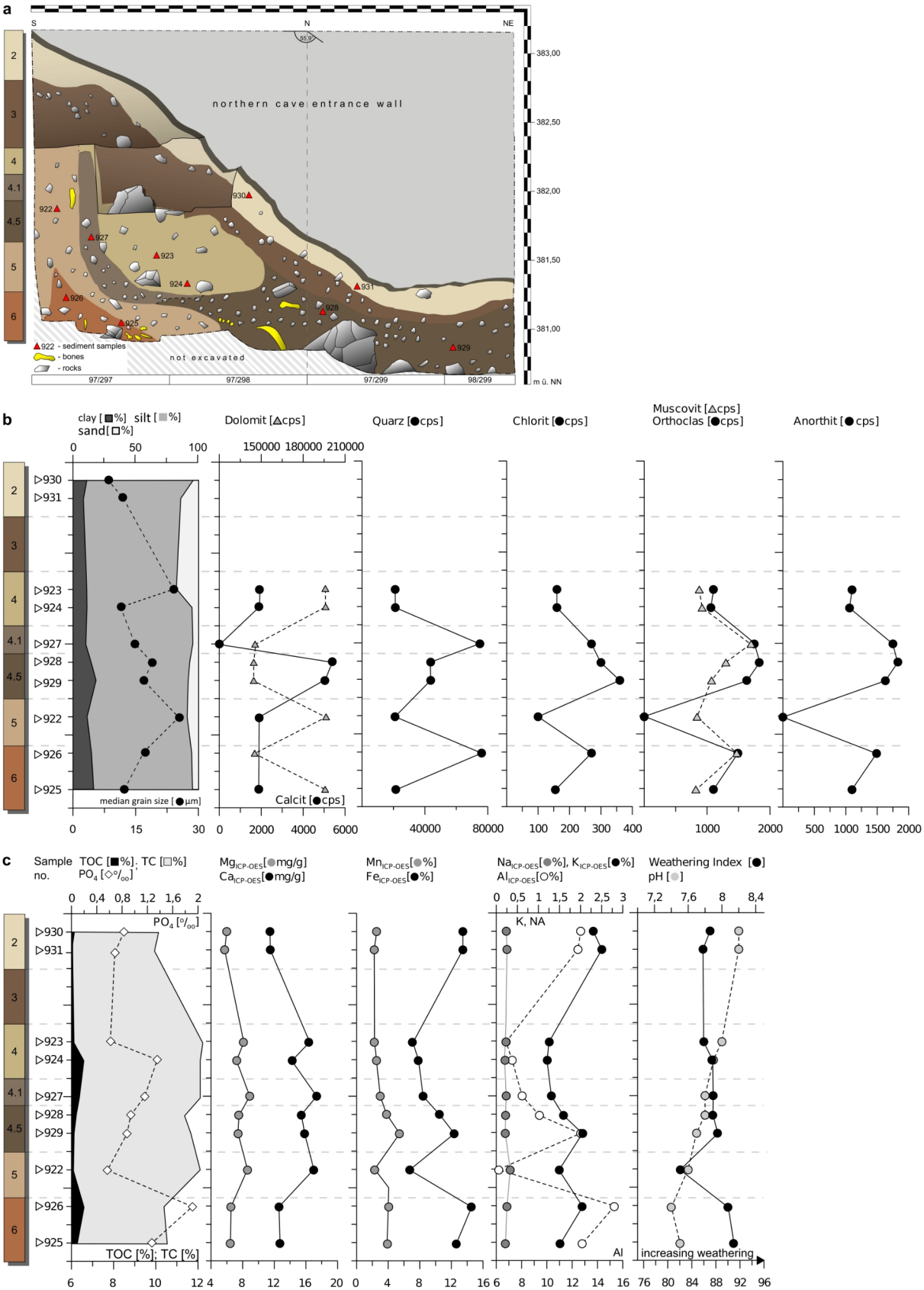

Supplementary Figure 5. Einhornhöhle. Locations of the sediment samples in the west section and results of sediments analyses. **a** Sample locations. **b** Grain size and mineral analyses. **c** Carbon and element analyses as well as Weathering Index (WI) after [68] and pH values.

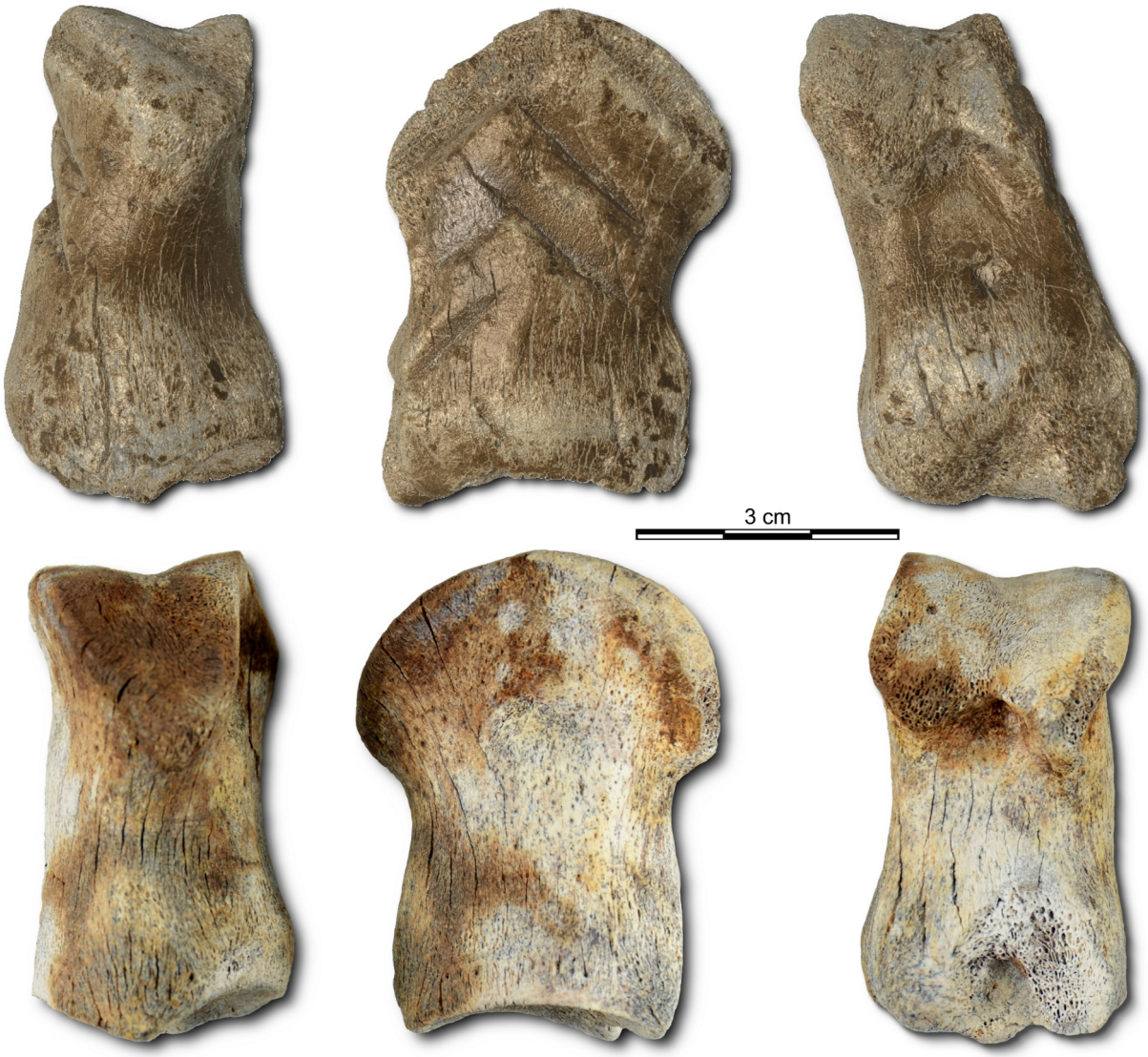

Supplementary Figure 6. Einhornhöhle. Comparison between the incised giant deer second phalanx (inv. no. 46999448-423) (top) and the unmodified giant deer second phalanx (inv. no. 48937021-0254) (bottom). The lateral views of the unmodified bone are mirrored for easier comparison.

Supplementary Figure 7. Einhornhöhle. Modified bones. **a** *Bos/Bison sp.* (Aurochs/Bison) left humerus shaft from layer 4.5. The cortical surface is heavily altered by roots. The central area bears cut marks associable to slicing for meat and butchering activities. **b** *Cervus elaphus* (red deer) right metacarpal from layer 6. Cut marks transversal to the main axes relate to slicing for meat. **c** *Cervus elaphus* (red deer) right metatarsal from layer 6. The marked pits along the main axes are carnivore bite marks. The bone was sampled for aDNA analyses.

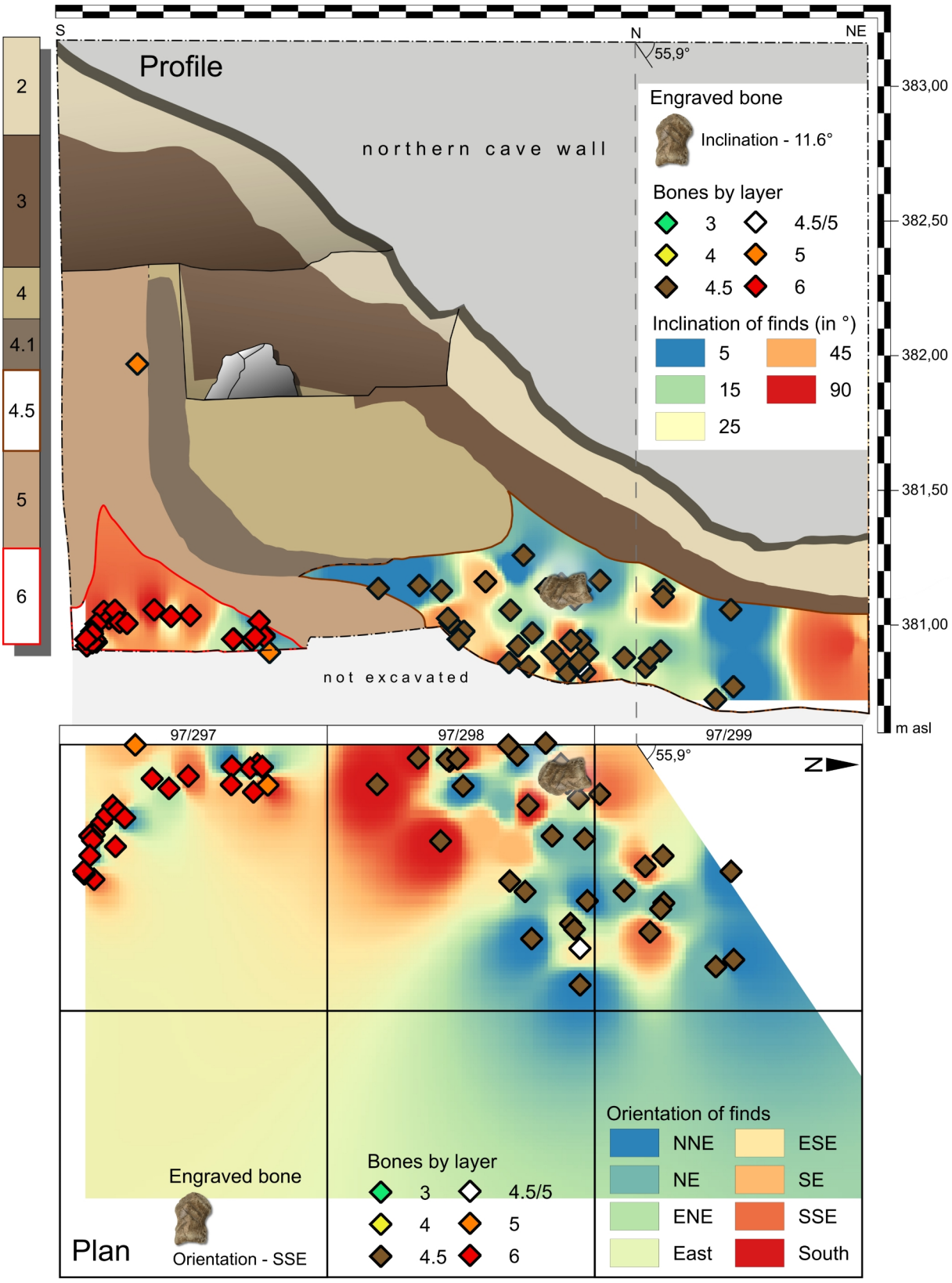

Supplementary Figure 8. Einhornhöhle. Inclination and orientation data of 70 individual bones from the cave entrance area (Area 4). Note low inclination levels near the engraved item. Grid in plan is 1m². Inverted Distance Weighting (IDW) in QGIS 3.8.2 was used to calculate inclination and orientation.

Supplementary Figure 9. Einhornhöhle. Bone accumulation discovered in the north-western corner of the excavation area in layer 4.5 (Figure 3 in main text). **a** The bone accumulation includes a cave bear skull, mandible and long bones. **b** The two cervid shoulder blades were found on top of each other just behind the cave bear skull to the west. Red circles in **a** and **b** indicates approximate position of the incised giant deer 2nd phalanx found below the two shoulder blades.

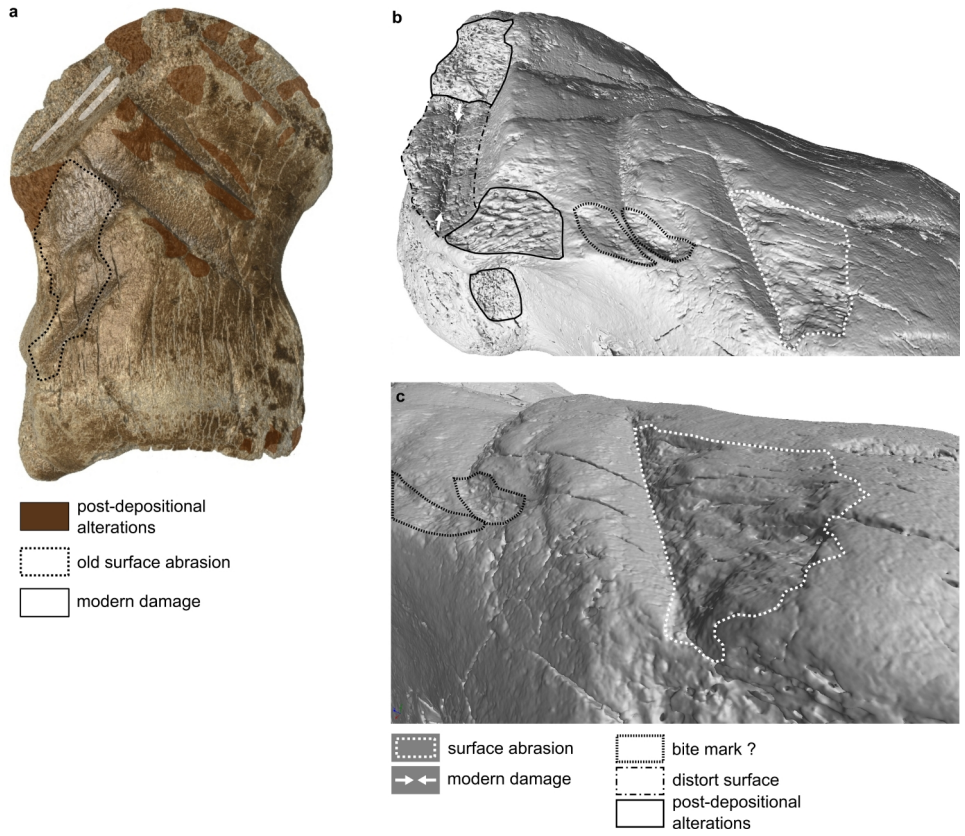

Supplementary Figure 10. Einhornhöhle. Post-depositional alterations on the engraved bone (inv. no. 46999448-423). **a** Alterations visible on the whole surface. **b** Detail of surface alterations on the left side of the phalanx (lines 1-3). **c** Close-up of line 1. See Figure 2 in the main text for line numbering.

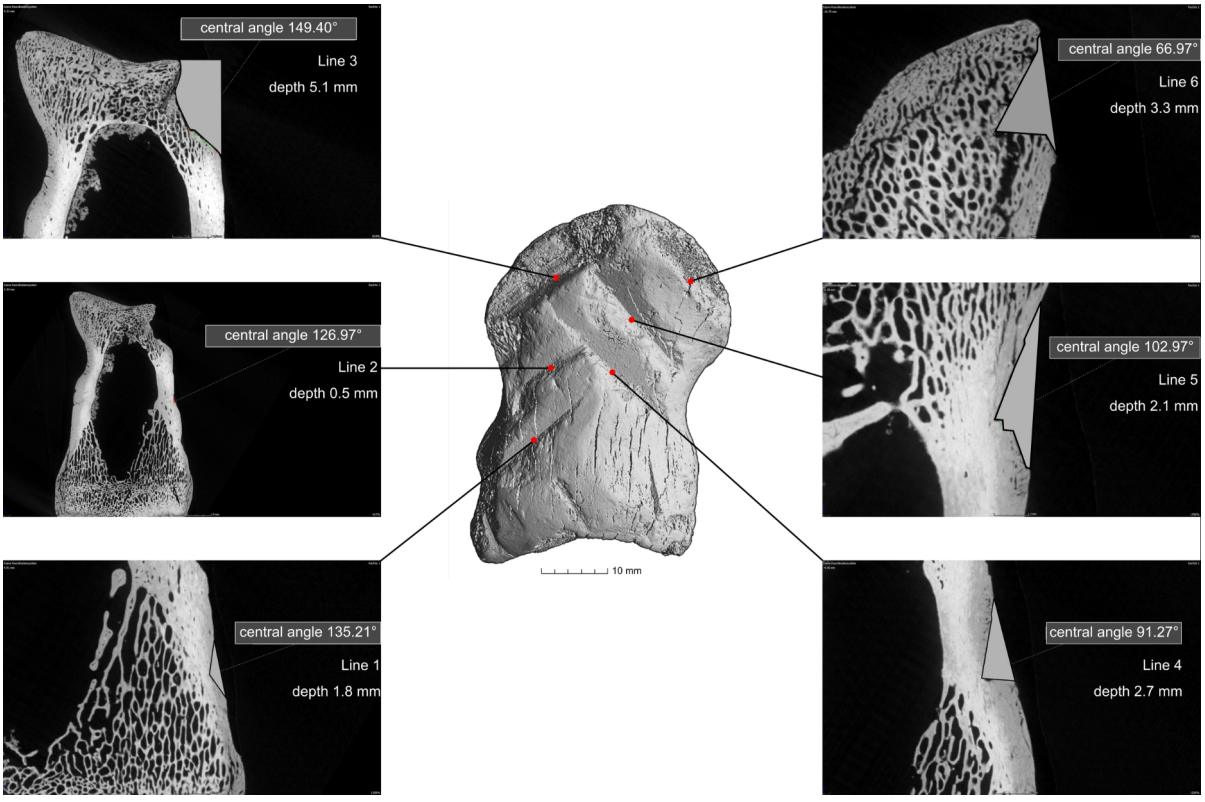

Supplementary Figure 11. Einhornhöhle. Depth and mass loss of the six major engravings on the incised bone Einhornhöhle (inv. no. 46999448-423). Surfaces of incisions nos. 3 and 6 are slightly affected by post-depositional alterations, so that preserved depths and profiles may deviate from original ones.

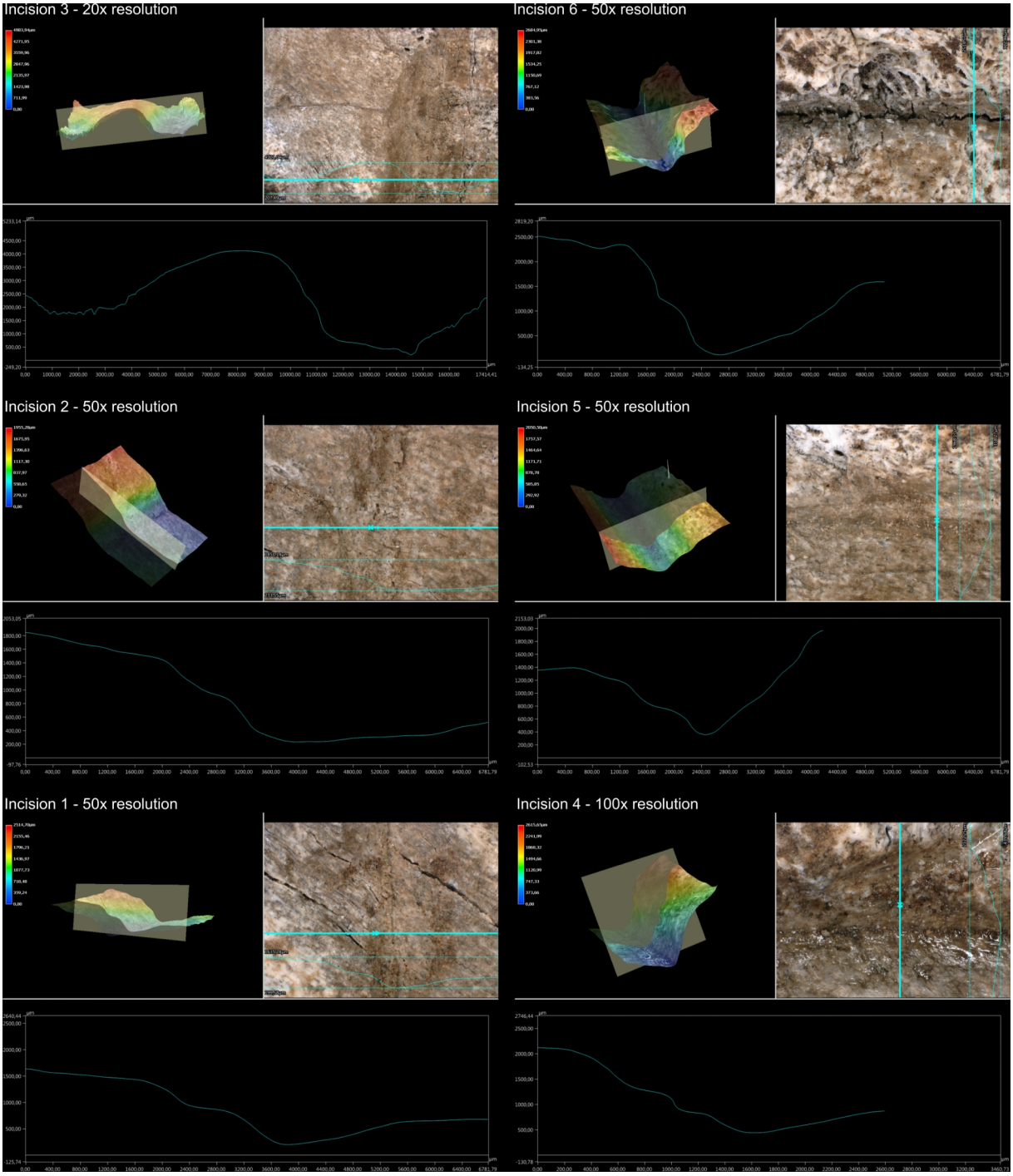

Supplementary Figure 12. Einhornhöhle. 3D Reflected Light Microscopy images, micro-topography and profiles of lines 1-6 of the engraved bone (inv. no. 46999448-423) from Einhornhöhle. For lines 3 and 4 two profiles are displayed and their difference represented by red and blue colours.

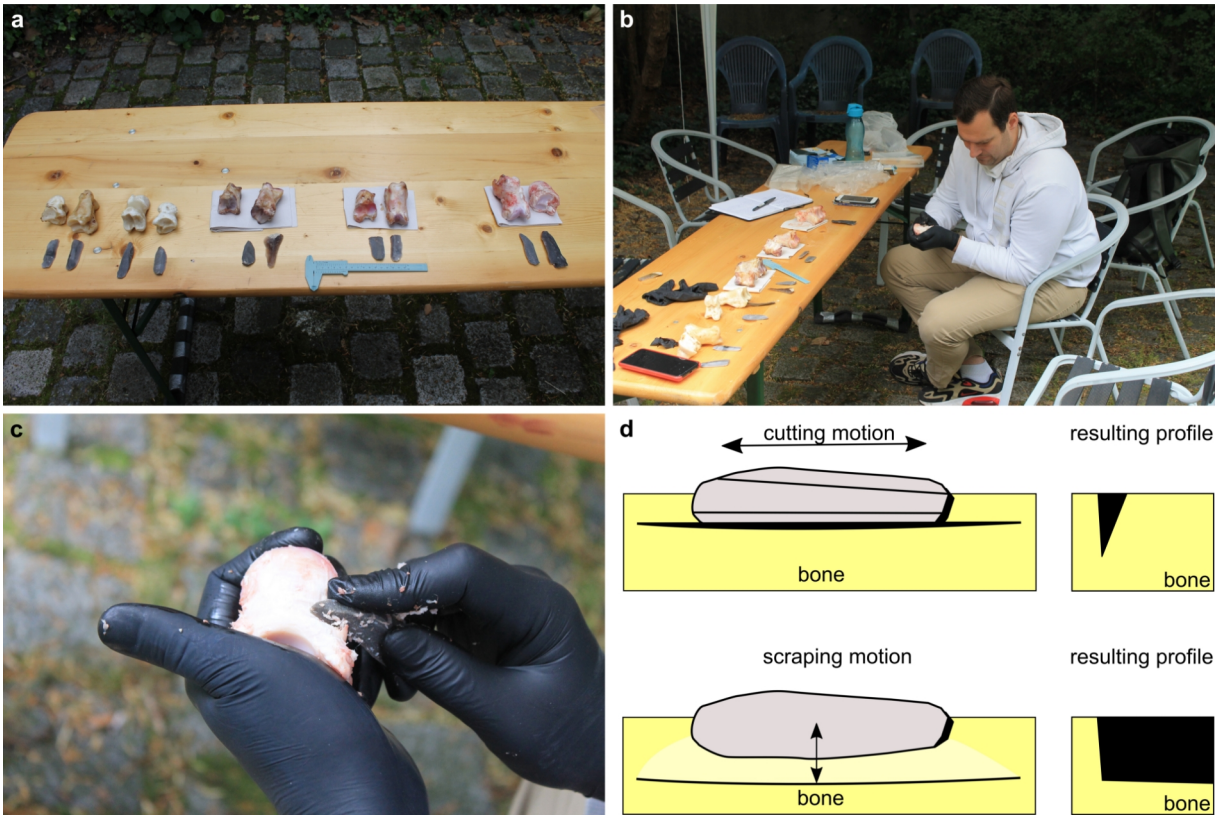

Supplementary Figure 13. Einhornhöhle. Bone carving experiment. **a** Set-up of the phalanges and blades used in the experiment. From left two right: bone cooked 1x, bone cooked 2x, open air dried bone, room dried bone, and fresh bone. **b** Body posture during the experiment. **c** Hand gesture when cutting into the bone tissue creating vertical surfaces. **d** Schematic representation of the cutting and scarping motions performed during the experiment.

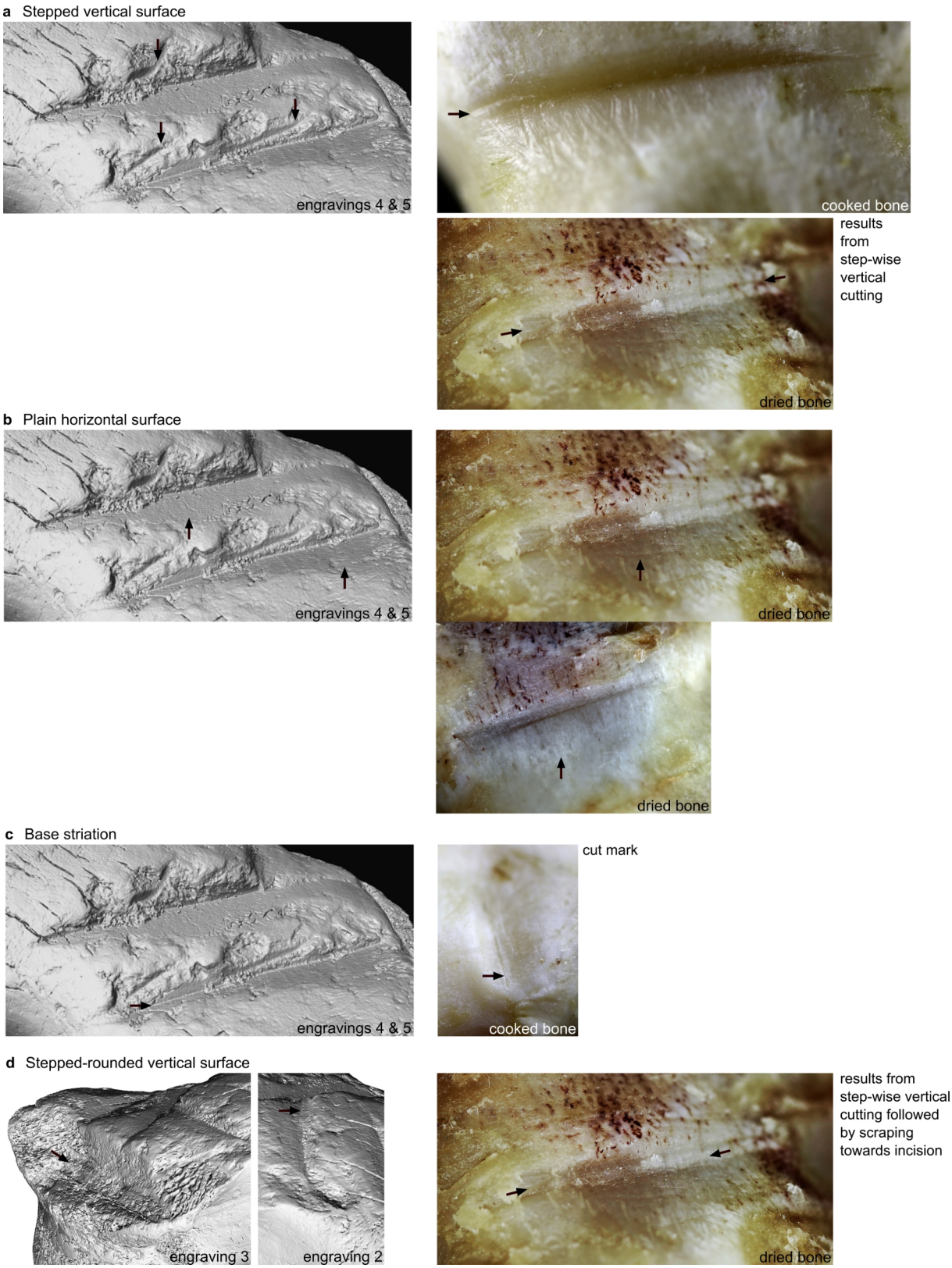

Supplementary Figure 14. Einhornhöhle. Characteristic features observed on engravings of the giant deer phalanx from Einhornhöhle (inv. no. 46999448-423) replicated in our experimental study. **Left** the engraved phalanx. **Right** the experimental bovine phalanx.

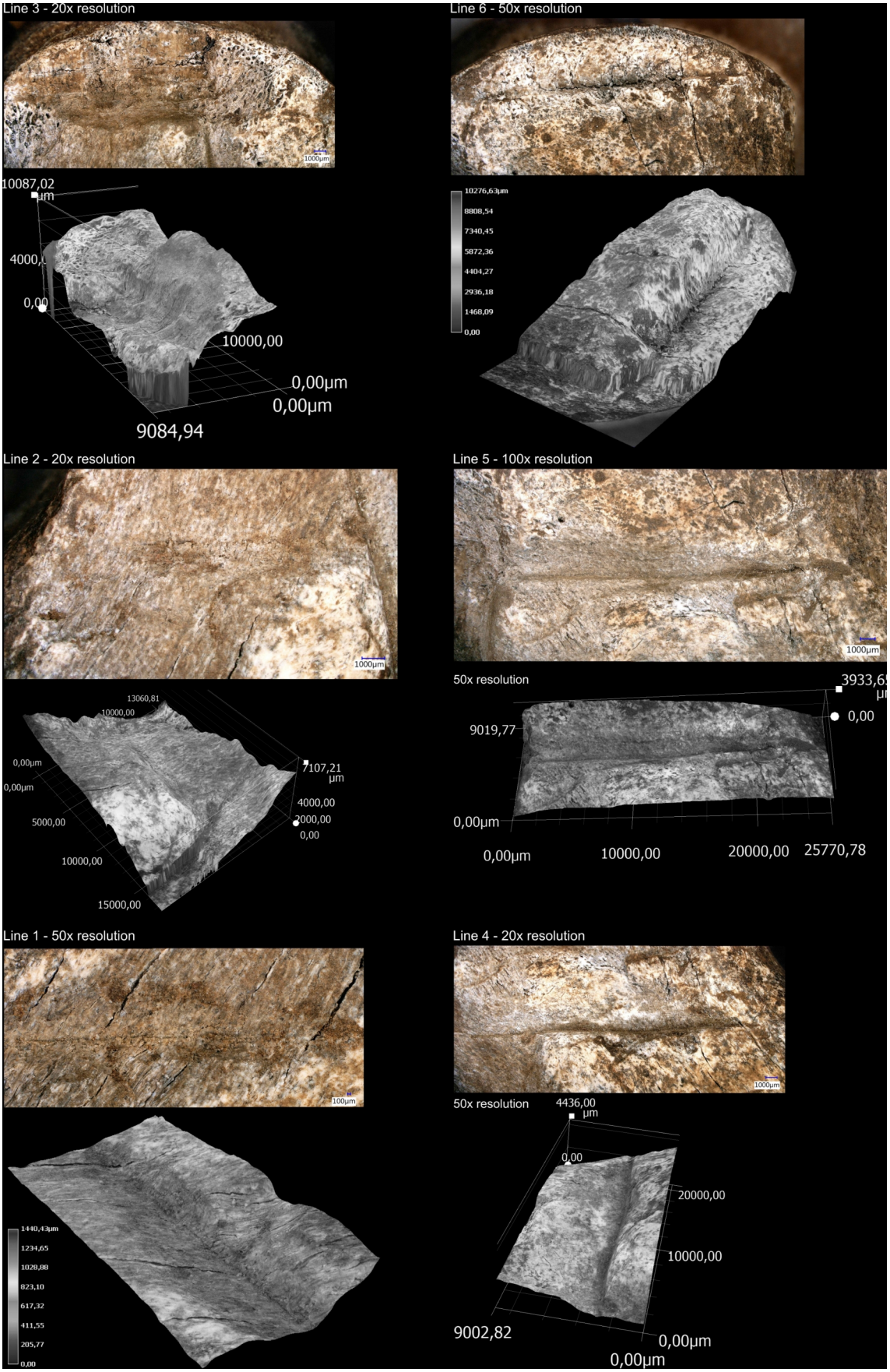

Supplementary Figure 15. Colour-greyscale image of Figure 4 in the main text. 3D digital microscopy images of the carved bone from Einhornhöhle (inv. no. 46999448-423). Stitched images of lines 1-6 at different resolutions and micro-topography images.

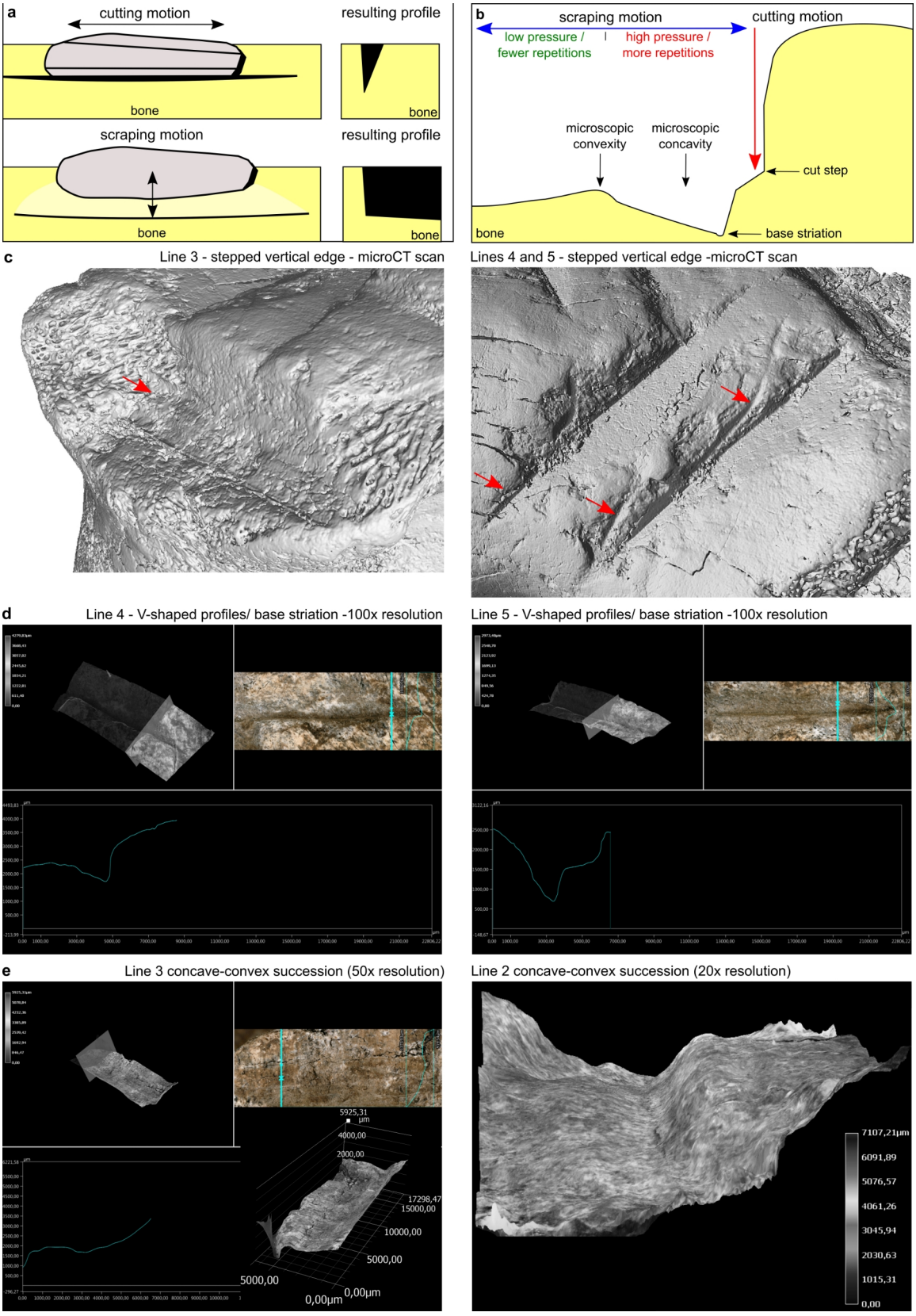

Supplementary Figure 16. Colour-greyscale image of Figure 5 in the main text. Micro-traces of lines 1-6. **a** Schematic representation of the cutting and scraping gestures applied during the experiment. **b** Schematic representation of micro-traces observed on lines 1-6. **c** Stepped vertical edges of lines 3-5. **d** Base striations of lines 4-5 displayed as V-shaped profiles. **e** Succession of concave-convex horizontal surfaces of lines 2-3.

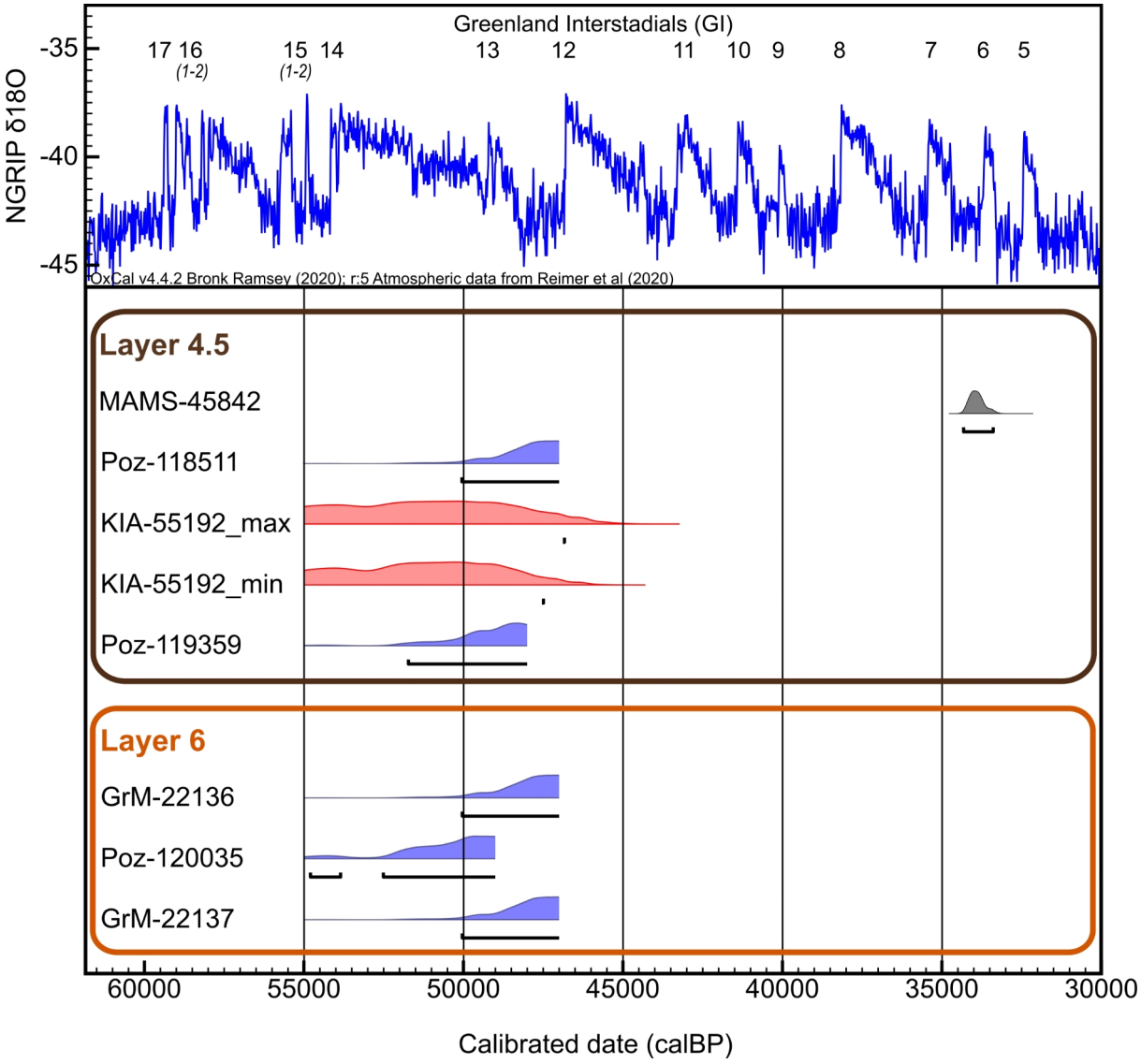

Supplementary Figure 17. Einhornhöhle. Calibrated radiocarbon ages (95.4 % probability) from cave entrance plotted against the NGRIP climate curve. Red age ranges: Engraved bone (inv. no. 46999448-423). Radiometric date was calibrated twice using different standard deviations, i.e. +2,800 (KIA-55192_max) and -2,100 (KIA-55192_min). Blue age ranges: accepted dates (with infinite or older-than ages). Grey age range: outlier. Radiocarbon dates were calibrated using OxCal v4.4.2 [61] and the IntCal20 atmospheric curve [62]. Minimum ages (e.g >45 ka BP) have been calibrated with 1 ka standard deviation.

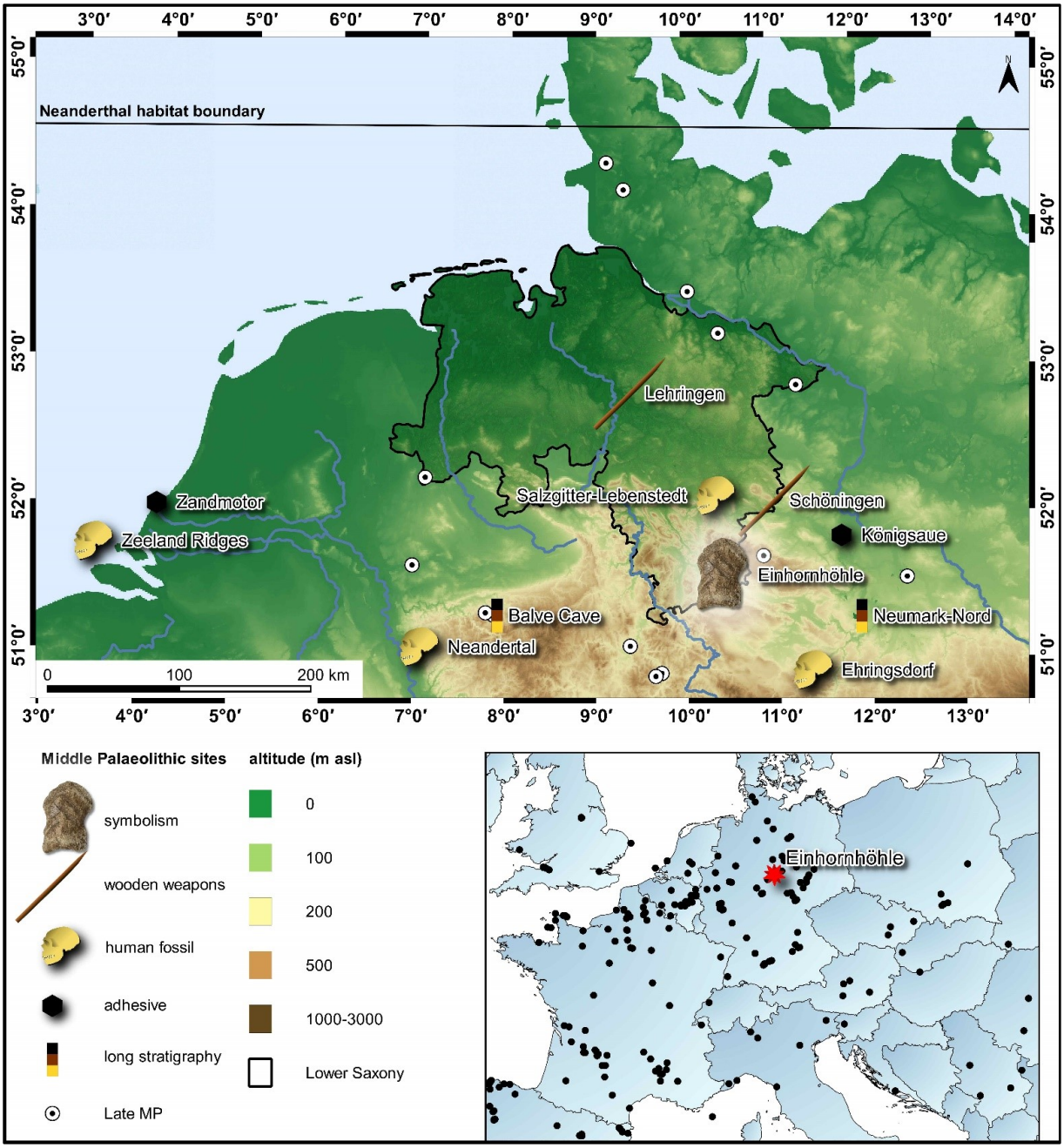

Supplementary Figure 18. Location of Einhornhöhle and further important Late Lower/ Middle Palaeolithic sites in northern Central Europe. Late MP stands for Late Middle Palaeolithic (MIS 5-3).

Supplementary Tables

Supplementary Table 1. Einhornhöhle. Faunal remains from layer 4.5 including the number of identified specimens (NISP) and its aggregates, and the associated bone surface modifications: AM, anthropogenic modification; pAM, potential anthropogenic modification; CM, carnivore modification; pCM, potential carnivore modification.

	NISP	AM	pAM	CM	pCM
Ungulates					
Bison sp.	4	0	0	4	0
Bos/Bison sp.	6	1	0	3	0
Megalocerus giganteus	12	1	0	1	0
Cervus elaphus	3	0	0	0	0
Very large ungulate	3	0	1	0	2
Large ungulate	2	0	1	1	0
Carnivora					
Ursus sp.	29	3	9	22	2
Gulo gulo	2	0	0	2	0
Vulpes vulpes	1	0	0	0	0
Large carnivore	4	0	0	2	0
Small carnivore	2	0	0	0	0
Indeterminate					
Medium mammal	29	1	0	13	0
Small or medium mammal	1	0	0	0	0
Small mammal	1	0	0	0	1
Total	99	6	11	48	5

Supplementary Table 2. Einhornhöhle. Weathering stages and corresponding NISP and %NISP.

Weathering stage	**NISP**	**%NISP**
No modification	4	4.2
Fine linear cracks	23	24.9
Open linear cracks	27	27.1
Many cracks and initial exfoliation	30	31.3
Medium exfoliation and flaking	5	5.2
Advanced exfoliation and flaking	6	6.3
Chemical weathering	1	1

Supplementary Table 3. Einhornhöhle. Surface angles between engravings 1-6 on phalanx (inv.-no. 46999448-423).

engravings 1 and 4	92.3°
engravings 2 and 4	100.5°
engravings 3 and 4	96.2°
engravings 3 and 5	94.2°
engravings 3 and 6	94.1°

Supplementary Table 4. Einhornhöhle. Central profile angles of engravings 1-6 on phalanx (inv.-no. 46999448-423).

engraving 1	135.2°
engraving 2	127.0°
engraving 3	149.4°
engraving 4	90.7°
engraving 5	103.0°
engraving 6	66.8°

Supplementary Table 5. Einhornhöhle. Results of experimental study.

	Bone 1	**Bone 2**	**Bone 3**	**Bone 4**	**Bone 5**
Preparation	as fresh	room dried	open air dried	1x cooked	2x cooked
Carving time (mins.)	25	20	23	16	11
Vertical cut	success	success	success	success	success
Horizontal plane	no	difficult	difficult	success	success
Groove depth	no	1 mm	1 mm	2 mm	2 mm
Workability	barely workable	difficult	difficult	easy	very easy
Rating	failure	partial success	partial success	success	success

Supplementary Table 6. Einhornhöhle. Metric data and macroscopic wear of blades used during the cutting and scraping experiment. **for fresh bone, only one blade was used because the bone was hardly workable.*

Blade No.	**Length (mm)**	**Width (mm)**	**Thickness (mm)**	**Weight (g)**	**Bone condition**	**Macroscopic use-wear**
1	68	22	7	10.5	as fresh*	hardly any edge wear
2	57	19	7	8.4	room dried	Partially well-developed, discontinuous, splintered edges
3	52	24	7	8.7	room dried	weakly developed, but

						continuous along both edges
4	68	32	7	12.0	open air dried	discontinuous, splintered edges
5	51	23	7	8.6	open air dried	well-developed along both edges
6	62	22	6	9.6	1x cooked	well-developed, along part of edge
7	68	20	8	13.6	1x cooked	well-developed along whole edge
8	62	20	7	7.2	2x cooked	well-developed over parts of both edges
9	77	17	7	8.2	2x cooked	well-developed over parts of both edges

Supplementary Table 7. Einhornhöhle. Samples submitted for radiometric dating and their context information. Samples are listed by altitude in descending order. **unsuccessful dating attempts are issued without LabID by CIO.*

LabID	**Field-ID**	**layer**	**easting**	**northing**	**altitude**	**find type**	**material**	**class**	**human impact**
Poz-118511	46999448-396	4.5	97.171	298.296	381.144	single plotted	charcoal	pinus sp.	-
MAMS-45842	46999448-971_1	4.5	96.883	298.760	381.141	single plotted	bone, mandible	indet.	no
MAMS-45843	46999448-971_2	4.5	96.883	298.760	381.141	single plotted	bone, rib	indet.	no
KIA-55192	46999448-423	4.5	97.077	298.853	381.139	single plotted	bone, phalanx	cervid	engraved
Poz-119359	46999448-402	4.5	97.238	298.268	381.127	bulk find	charcoal	pinus sp.	-
GrM-x*	46999448-904	4.5	97.067	298.458	381.012	single plotted	bone, phalanx	indet.	cut mark
GrM-22136	46999448-383	6	97.218	297.615	380.990	single plotted	bone, metatarsus	cervid	cut mark
Poz-120035	46999448-659	6	97.138	298.313	380.945	single plotted	charcoal	pinus sp.	-
GrM-22137	46999448-377	6	97.350	297.705	380.904	single plotted	bone, phalanx	cervid	cut mark

Supplementary Table 8. Einhornhöhle. Radiometric dates from Einhornhöhle's cave entrance. Age estimates are listed by altitude in descending order. ^{14}C-age estimates were calibrated with the OxCal 4.4 calibration software using the IntCal20 calibration curve [61-62]. **unsuccessful dating attempts are issued without LabID by CIO*.

LabID	**δ13C AMS [‰]**	**C [%]**	**Collagen [%]**	**C:N**	**pMC**	**^{14}C-age (BP)**	**sd (±)**	**Cal 2-sigma (calBP)**	**comment**
Poz-118511	-	-	-	-	-	>45,000	-	-	minimum age
MAMS-45842	-22.9	17.4	0.2	3.3		29,340	180	34,325 – 33,395	low collagen yield
MAMS-45843	-	-	-	-	-	-	-	-	no collagen preserved
KIA-55192	-20.3 ± 0.2	41 ± 2	4.0		0.26±0.08	47,800	+2800/-2100	>55,000 – 47,492	
Poz-119359	-	-	-	-	-	>46,000	-	-	minimum age
GrM-x*	-	32.7	0.17	2.6	-		-	-	collagen yield too low
GrM-22136	-19.77	41.4	1.5	3.1	-	>45,000	-	-	minimum age
Poz-120035	-	-	-	-	-	>47,000	-	-	minimum age
GrM-22137	-19.96	39.9	0.8	3.1	-	>45,000	-	-	minimum age

Supplementary Table 9. Neanderthal sites with major art objects or symbolic behaviour proposed. *(MP) = Middle Palaeolithic, (CP) = Châtelperronian*

Site	Region	Type	Calendric age (ka BP)	Method	Description/ Comment	Reference
Cova Foradada (CP)	NE-Spain	personal ornaments	>39	C14	imperial eagle phalanges, minimum age	[36]
Combe-Grenal (MP)	SW-France	personal ornaments	90	-	Feathers, various birds of prey	[90]
Grotte du Renne (CP)	C-France	personal ornaments	40-45	C14	drilled and grooved teeth and bone pendants, Châtelperronian, 40-45 ka calBP	[31]
Quincay (CP)	C-France	personal ornaments	-	-	drilled tooth pendant, Châtelperronian, 40-45 ka calBP	[30]

Krapina (MP)	Croatia	personal ornaments	130	ESR, U-Th	white-tailed eagle claws with cut marks, also evidence for Neanderthal cannibalism	[34]
Les Fieux (MP)	SW-France	personal ornaments	40-60	-	golden eagle claws with cut marks	[90]
Mandrin Cave (MP)	SE-France	personal ornaments	50.0	C14	eagle talons	[35]
Rio Secco Cave (MP)	N-Italy	personal ornaments	48.0-49.1	C14	eagle talons	[35]
Grotta di Fumane (MP)	N-Italy	personal ornaments	42-2-44.8	C14	Feathers, various birds of prey	[33]
Ardales (MP)	SW-Iberia	cave art	33-70	U-Th	ochre paint on speleothem, oldest age is minimum age	[37]
La Pasiega (MP)	N-Iberia	cave art	50-80	U-Th	ochre painting, red symbol, oldest age is minimum age	[37]
Maltravieso (MP)	SW-Iberia	cave art	41-70	U-Th	hand stencil, oldest age is minimum age	[37]
Einhornhöhle (MP)	N-Germany	engraving	>55-47.5	C14	Giant deer phalanx with geometric pattern, directly dated, in agreement with further dates	this study
Kiik-Koba (MP)	Crimea	engraving	35-37	C14	flint artefact with sub-parallel line carvings, associated with child burial	[41]
Kůlna, levels 6-11 (MP)	Moravia	engraving	40-80	U-Th, OSL, C14	15 bones with engraved line patterns, potentially unintentional cut marks	[91, 92]
La Ferrassie (MP)	SW-France	engraving	60-70	-	shaft bone with four parallel line bundles, associated with burial 1, old excavation, Peyrony 1934	[30]
Les Pradelles (MP)	S-France	engraving	60-70	U-Th, TL	parallel deep incisions interpreted as numbering system	[93]
Oldisleben (MP)?	Central Germany	engraving	-	-	three bones with engraved lines, finds from open cast mine, no primary context	[94]
Prolom II (MP)	Crimea	engraving	-	-	line engravings on three bones and teeth, radiocarbon ages too young	[45, 92]
Biqat Quneitra (MP)	Golan Heights	engraving	53.9 ± 5.9	ESR	one engraved bone and one rock, circles	[44]
Nesher Ramla (MP)	Israel	engraving	c. 120	OSL/TL	engraved shaft bone with six sub-parallel lines, Homo sapiens or Neanderthals?	[46]

Zaskalnaya VI (MP)	Crimea	engraving	38-43	C14	a raven radius with eight parallel notches	[41]
Cueva Antón (MP)	S-Iberia	shell bead	>50	C14	perforated and pigment stained, minimum age, >60 km transport	[95]
Cueva de los Aviones (MP)	S-Iberia	shell bead	>50	C14	perforated and pigment stained, minimum age; site near coast	[95]
Grotta di Fumane (MP)	N-Italy	shell bead	45-47.6	C14	single shell, ochre stained, Miocene shell from >100 km distance	[96]
Axlor rock-shelter (MP)	NE-Iberia	pecked pebbles	>47.5	C14	split sandstone pebble with pecked cross, minimum age	[97]
Gorhams Cave (MP)	Gibraltar	rock carving	30-39	C14	chess board-like rock carving, oldest age is minimum	[43]
La Ferrassie (MP)	SW-France	rock carving	60-70	-	cupules pecked into rock surface, covered a child burial, old excavation, Peyrony 1934	[30]

Supplementary References

68. Nesbitt, H. W. & Young, G. M. Early Proterozoic climates and plate motions inferred from major element chemistry of lutites. *Nature* **299**, 715-717 (1982).
69. McCuaig Balkwill, D. & Cumbaa, S. L. *A Guide to the Identification of Postcranial Bones of Bos taurus and Bison bison*. (Canadian Museum of Nature, Syllogeus 71, Ottawa, 1992).
70. Brown, C. L. & Gustafson, C. E. *A Key to Postcranial Skeletal Remains of Cattle / Bison, Elk, and Horse*. (Reports of investigations 57, Washington State University, 1979).
71. Tillet T. & Binford L. R. *L'Ours et l'Homme.* (Actes du colloque d'Auberives-en-Royans 1997, Université de Liége, ERAUL 100, 2002).
72. Grayson, D. K. *Quantitative Zooarchaeology.* (Topics in the Analysis of Archaelogical Faunas: A volume in Studies in Archaeology, Academic Press, 1984).
73. Stiner, M. C. *Honor among Thieves: A Zooarchaeological Study of Neandertal Ecology*. Princeton University Press, Princeton, 1994).
74. Lyman, R. L. *Quantitative Paleozoology. 2nd Edition*. (Cambridge University Press, New York, 2012).
73. Domínguez Rodrigo, M., de Juana, S., Galan, A. B. & Rodríguez, M. A new protocol to differentiate trampling marks from butchery cut marks. *J. Archaeol. Sci.* **36**, 2643–2654 (2009).
75. Bello, S. M., Parfitt, S. A. & Stringer, C. Quantitative micromorphological analyses of cut marks produced by ancient and modern handaxes. *J. Archaeol. Sci.* **36**, 1869–1880 (2009).
76. Fernandez-Jalvo, Y. & Andrews, P. *Atlas of Taphonomic Identifications*. (Vertebrate Paleobiology and Paleoanthropology, Springer, New York, 2016).

77. Lyman, R. L. *Vertebrate Taphonomy.* (Cambridge University Press, Cambridge, 1994).
78. Anonymous. *DIN EN 1334. Charakterisierung von Schlämmen - Bestimmung von Spurenelementen und Phosphor - Extraktionsverfahren mit Königswasser; Deutsche Fassung EN 13346*: 2000. (Beuth Verlag, Berlin, 2001).
79. Anonymous. *DIN ISO 10390, 2005. Bodenbeschaffenheit - Bestimmung des pH-Wertes. Deutsche Fassung ISO 10390: 2005.* (Beuth Verlag, Berlin 2005).
80. Alunni-Perret, V. *et al.* Scanning electron microscopy analysis of experimental bone hacking trauma. *J. Forensic Sci,* **50(4)**, 796–801 (2005).
81. Lewis, J. E. Identifying sword marks on bone: criteria for distinguishing between cut marks made by different classes of bladed weapons. *J. Archaeol. Sci.* **35**, 2001–2008 (2008).
82. Osipowicz, G. Bone and antler: softening techniques in prehistory of the North Eastern Polish Lowlands in the light of experimental archaeology and micro-wear analysis. *EuroREA* **4**, 1–22 (2007).
83. Newcomer, M. Experiments in Upper Palaeolithic bone work. In: Camps-Faber, H. (ed.) *Méthodologie Appliqué A L'industrie de l'os préhistorique* (Colloque international du CNRS 569, Naples, 291–301, 1976).
84. Longin R (1971) New Method of Collagen Extraction for Radiocarbon Dating. *Nature* **230**, 241–242.
85. Stenström, K., Skog, G., Georgiadou, E., Genberg, J. & Johanson, A. *A Guide to Radiocarbon Units and Calculations* (Lund University, Lund, 1–17, 2011).
86. Stuiver, M. & Polach, H. A. Discussion: Reporting of 14C data. *Radiocarbon* **19**, 355–363 (1977).
87. Huels, M., van der Plicht, J., Brock, F., Matzerath, S. & Chivall, D. Laboratory intercomparison of Pleistocene bone radiocarbon dating protocols. *Radiocarbon* **59(5)**, 1543–1552 (2017). doi:10.1017/RDC.2017.23
88. Dee, M., Palstra, S., Aerts-Bijma, A., Bleeker, M., De Bruijn, S., *et al*. Radiocarbon Dating at Groningen: new and updated chemical pretreatment procedures. *Radiocarbon* **62,** 63–74 (2020). doi:10.1017/RDC.2019.1013
89. Morin, E. & Laroulandie, V. Presumed Symbolic Use of Diurnal Raptors by Neanderthals. *PLOS ONE* **7(3)**, e32856. https://doi.org/10.1371/journal.pone.0032856
90. Neruda P (2010). Economic behaviour and mental capacity of Neanderthals. In: Fridrichová-Sýkorová, I. (ed.). *Ecce Homo: In Memoriam Jan Fridrich (*Knižnice České společnosti archaeologické 1, Krigl, Prague, 111–129, 2010).
91. Vermeersch, P. Radiocarbon Palaeolithic Europe Database Version 26. http://ees.kuleuven.be/geography/projects/14c-palaeolithic/index.html (2020).
92. d'Errico, F. *et al.* From number sense to number symbols: an archaeological perspective. *PHILOS T R SOC B* **373**, 20160518 (2018). http://dx.doi.org/10.1098/rstb.2016.0518
93. Bednarik, R. G. The Middle Palaeolithic engravings from Oldisleben, Germany. *Anthropologie* **44(2)**, 113–121 (2006).
94. Zilhão, J., Angelucci, D. E., Badal-García, E., d'Errico, F., Daniel, F. *et al.* Symbolic use of marine shells and mineral pigments by Iberian Neandertals. *PNAS* **107**, 1023–1028 (2010).

95. Peresani, M., Vanhaeren, M., Quaggiotto, E., Queffelec & d'Errico, F. An Ochered Fossil Marine Shell from the Mousterian of Fumane Cave, Italy. *PLOS ONE* **8**: e68572. (2013).
96. Garcia García-Diez, M., Ochoa Fraile, B., Barandiarán Maestu, I. Neanderthal graphic beahvior. *J. Anthropol. Res.* **69**, 397–410 (2013).